Sciforce

Journal of Organic Chemistry Synthesis and Process Development
Journal homepage: www.sciforce.org

Simple phenylene-bridged D-π-A type photosensitizers for DSSC application: Synthesis, optical, electrochemical and theoretical studies

Kavya S. Keremane[a], and Airody Vasudeva Adhikari[a,b,*]

[a]*Organic Materials Laboratory, Department of Chemistry, National Institute of Technology Karnataka, Surathkal, Mangalore-575025, India*

[b]*Yenepoya Research Centre, Yenepoya deemed to be University, Deralakatte, Mangalore-575018, India*

ARTICLE INFO

ABSTRACT

Herein, we report the design and synthesis of two new phenylene-bridged D-π-A configured organic molecules N_{1-2} carrying two different anchors and the same donor unit, as potential sensitizers for DSSC application. In the new design, a simple *O*-alkyl substituted phenyl group acts as a donor scaffold, cyanovinylene, and phenylene systems serve as π-spacers, while cyanoacetic acid and barbituric acid units function as electron acceptor/anchoring moieties. The current work also highlights their structural, photophysical, electrochemical, and theoretical investigations, including evaluation of their structure-property relationships. The optical results revealed that chromophores N_{1-2} display λ_{abs} and λ_{emi} in the range of 400-420 nm and 550-570 nm, *respectively*, with a bandgap in the order, 2.51-2.59 eV. Their quantum chemical simulations have provided an insight into the predictions of their structural, molecular, electronic, and optical parameters. Further, the results showcased that the dyes possess all the pre-requisites to act as sensitizers in dye-sensitized solar cells (DSSCs). Conclusively, the study furnishes a deeper understanding of the intricacies involved in the structural modification of phenylene-based dyes for achieving better performance in DSSCs.

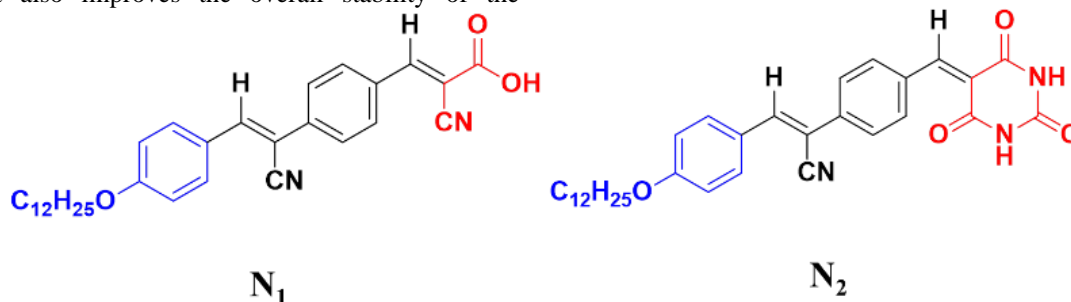∗Corresponding author. e-mail: avachem@gmail.com

1. Introduction

Over the past three decades, the quest for low-cost energy production from renewable energy resources has gained much attention to address the problem of world energy crisis.[1–4] The new third-generation photovoltaic device, especially dye-sensitized solar cells (DSSCs) have attained much interest as a new generation sustainable photovoltaic devices, mainly due to their ability to convert direct sunlight into electricity at low fabrication cost, and easy manufacturing process when compared to conventional *p-n* junction solar cells.[5,6] Typically, DSSCs are composed of sandwich structure: dye-adsorbed wide bandgap metal-oxide-semiconductor electrode (TiO₂), a platinum counter electrode, filled with an electrolyte containing I⁻/I₃⁻ redox couple. In general, the working principle of DSSCs involves the absorption of photons by the sensitizers (dyes) to get excited and consequently injection of electrons into the conduction band (CB) of the TiO₂ followed by regeneration of the dye using the redox electrolyte.[7] Among all the components

of DSSCs, the photosensitizer (dye) plays a key role in enhancing power-conversion efficiency (PCE) of the cell. The sensitizers with appropriate HOMO-LUMO energy levels and light-harvesting ability may lead to satisfactory photoelectric conversion efficiency.[8] During the last decades, much effort has been made on developing new sensitizers to enhance the overall performance of the devices. Till date, the metal-organic complexes (Ru-based) have been shown to achieve a high PCE above 14 % under AM 1.5 irradiation.[9,10] Due to their high manufacturing cost, tedious synthetic methods, tricky purification steps, and environmental issues, metal-free organic dyes have been used as an alternative to replace them. These organic dyes overcome all the above-said drawbacks with their high molar extinction coefficient, better flexibility for structural control, environmental friendliness, and considerable efficiencies.[11-13] However, the *PCE* of these sensitizers is still low when compared to devices based on Ru-based dyes.

on the TiO$_2$ surface. In the literature, a wide range of design strategies have been reported for the development of effective organic sensitizers/co-sensitizers.[14] One such approach is making use of a simple D-π-A strategy, where D/A and π refer to the electron donor/acceptor and π-bridge groups, respectively. Interestingly, various electron-rich molecules such as triphenylamine, coumarin, carbazole, indole, *etc.* act as a good donor, by pushing electrons to an electron pulling acceptor group like carboxylate or phosphonate, which facilitates strong grafting on the TiO$_2$ layer.[15,16] Generally, the geometry of the dye molecules largely correlates with certain factors such as *PCE*, the stability of the molecule, electron injection, dye regeneration, and recombination. One of the major reasons for the observed low *PCE* was the common problem associated with the dye, *viz.* aggregation and charge recombination. In order to suppress this, the introduction of long alkyl chains or a bulky group on donor moiety was found to be a useful strategy.[17,18] Normally, the introduction of conjugated π spacers between donor and acceptor moieties not only helps in enhancing electron conjugation but also improves the overall stability of the

Evidently, the photocurrent generation and hence the overall performance of DSSCs mainly depends on the structural properties of the dye and the amount of dye molecules adsorbed molecule. In several D-π-A architectures, phenylene-based aromatic systems were widely used as π-spacers because of their excellent stability, more effective conjugation, and electronic tunability.[19] Further, in the literature, cyanoacetic acid (CA) and barbituric acid (BA) are widely used as electron acceptors due to their excellent electron-withdrawing ability.[20,21]

Encouraged by this, in the present work, we have designed two new D-π-A configured organic chromophores **N$_{1-2,}$** carrying *O*-alkyl substituted phenyl group (dodecyloxyphenyl) as the electron donor, cyanovinylene together with phenylene system as the π-spacer, and cyanoacetic acid and barbituric acid groups as the electron acceptor/anchoring units. **Figure 1** portrays the chemical structures of **N$_{1-2}$**. These molecules were designed with the possible application in DSSCs as active sensitizers. Keeping in view of its cost-reduction, these molecules were synthesized conveniently by adopting simple synthetic methods, such as *N*-alkylation, Vilsmeier-Hack reaction and Knoevenagel condensation methods that gave high yield of the final product. **Scheme 1** outlines the synthetic methods followed for **N$_{1-2}$**.

Figure1. Chemical structures of D-π-A configured new dyes **N$_{1-2}$**

2. Material and methods

The starting materials such as 4-hydroxybenzaldehyde, 1-bromododecane, phenylacetonitrile, cyanoacetic acid, and barbituric acid were procured from Sigma-Aldrich, Alfa Aesar, and Spectrochem companies. All the solvents used in the reactions were of synthetic grade (Merck, LobaChemie, and Spectrochem companies) and they were purified by further drying and distillation process. All the reactions were carried under an inert (argon) atmosphere and the reaction completion was monitored by the TLC technique. The designed dyes were synthesized by using a standard synthesis protocol. The target dyes and their intermediates were purified using recrystallization or column chromatographic separation techniques. The melting points of synthesized molecules were recorded using the Stuart SMP10 digital melting point apparatus.[1] H NMR (400 MHz) spectra of synthesized molecules were recorded on the BrukerAvance (III) 400 MHz instrument by using DMSO-d$_6$ as a solvent. The FT-IR spectra were obtained using the Bruker FTIR Alpha spectrometer. The UV-Vis absorption spectra and photoluminescence spectra of **N$_{1-2}$** in *N,N*-dimethyl formamide

(DMF) solvent were recorded at room temperature by using the Analytik Jena SPECORD S 600 and Jasco FP 6200 spectrophotometers, *respectively*. Furthermore, in order to assess their experimental GSOP and ESOP values, the CV (cyclic voltammetry) measurements were performed in anhydrous acetonitrile solution with 0.1M tetrabutylammonium hexafluorophosphate [TBA] [PF$_6$] as a supporting electrolyte at a scan rate of 100 mVs^{-1}. The theoretical simulations, *viz.* density functional theory (DFT) and time-dependent density functional theory (TD-DFT), were performed for all the final molecules using the Turbomole V7.2 software package.

3. Experimental

3.1 Synthesis and characterization

The synthetic pathways of two new metal-free organic dyes **N$_{1-2}$** are shown in **Scheme 1.** The required alkoxy benzaldehyde **2** was synthesized from 4-hydroxybenzaldehyde (**1**) by reacting it with 1-bromododecane in presence of potassium carbonate. Subsequently, the aldehyde **2** was condensed with phenylacetonitrile to obtain the substituted phenyl acrylonitrile **3**

as an intermediate. Further, this intermediate was formylated using the standard Vilsmeier-Hack reaction protocol to yield precursor **4**. In the final step, the target molecules **N₁₋₂** were obtained by following the Knoevenagel condensation protocol, wherein the precursor **4** was condensed with an active methylene compound, *viz*. cyanoacetic acid and barbituric acid. All the
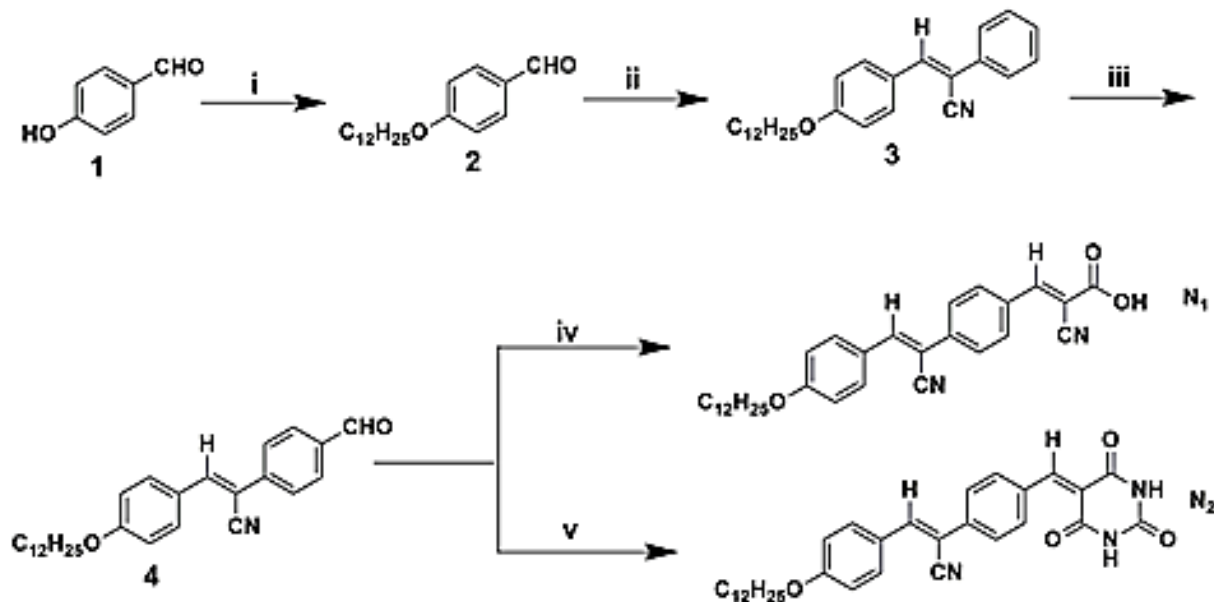
Scheme 1. Synthetic routes for the dyes **N₁₋₂**: (i) 1-Bromododecane, potassium carbonate, DMF, RT, 10 hours (ii) Phenylacetonitrile, sodium methoxide, methanol, RT, 6 hours (iii) POCl₃, DMF, RT, 12 hours (iv) Cyanoacetic acid, ammonium acetate, glacial CH₃COOH,110 °C, 10 hours (v) Barbituric acid, methanol, 60 °C, 10 hours.

synthesized compounds were purified using recrystallization or column chromatography techniques. The molecular structures of the newly synthesized target dyes and their intermediates were confirmed by using various spectroscopy methods (**Figure 2**) and elemental analysis.

3.2 Synthetic methods

Synthesis of intermediate 4-(dodecyloxy)benzaldehyde(2)

The starting material 4-hydroxybenzaldehyde (**1**, 1 eq) was dissolved in a minimum amount of DMF and stirred for 0.5 h and further potassium carbonate (3 eq) was added to the above mixture. Finally, 1-bromododecane (1.2 eq) was added to the above reaction mixture and was heated with stirring at 80 °C for 12 h. The reaction progress was monitored using TLC. After completion of the reaction, the reaction mixture was cooled, and poured into ice-cold water, and extracted with dichloromethane. The combined organic layer was dried using sodium sulphate and the solvent was removed under reduced pressure. Finally, the crude product was purified by the column chromatography method using 100-200 silica mesh (pet ether:ethyl acetate, 3:1, as eluent) to obtain the pure product as a colourless liquid. Yield: 89-91%.

Synthesis of intermediate (Z)-3-(4-(dodecyloxy)phenyl)-2-phenylacrylonitrile (3)

Intermediate **2** (1 eq) and phenylacetonitrile (1.2 eq) was slowly added to the round-bottomed flask containing freshly prepared sodium methoxide (1.8 eq, 50 mL) solution. The reaction mass was stirred at room temperature under argon atmosphere for 8 h. The bright yellow precipitate formed was filtered off, washed with cold methanol and finally, it was recrystallized from chloroform to give a fine yellow solid of **3**. Yield: 84-88%.

Synthesis of intermediate (Z)-3-(4-(dodecyloxy)phenyl)-2-(4-formylphenyl)acrylonitrile (4)

DMF (5 eq) and phosphorous oxychloride (5 eq) was mixed under argon atmosphere and stirred at –3 to 4 °C for 30 minutes in order to get white colouredVielsmeier salt. To this salt, the intermediate **3** (1 eq) in dichloroethane (2-3 mL) was added and stirring was continued at room temperature for 12 h. After completion of the reaction, the reaction mass was poured into ice-cold water and subsequently basified by using 5M NaOH solution. The precipitated solid was filtered and collected. The crude product was further purified by column chromatography (100-200 mesh and Hexane: EtOAc, 3:1 eluent) and finally, it was recrystallized from ethanol to get the pure dark orange-colored solid **4.** Yield: 85-86%.

Synthesis of (E)-2-cyano-3-(4-((Z)-1-cyano-2-(4-(dodecyloxy)phenyl)vinyl)phenyl)acrylic acid (N₁)

A mixture of intermediate **4**, (1 eq), cyanoacetic acid (1.2 eq), and ammonium acetate (10 eq) and glacial acetic acid (10-15 mL) was taken in a RB flask and refluxed for 12 h under argon atmosphere. The completion of the reaction was monitored using the TLC technique. After its completion, the reaction mixture was cooled to room temperature and was poured into ice-cold water. The solid obtained was filtered, washed with cold water, and finally, dried. The crude product was recrystallized from absolute methanol to get the pure product **N₁**.

Bright red solid, Yield: 83%, melting point: 240-242 ºC.**¹H NMR** (400 MHz, DMSO-d6, δ ppm): 11.33 (s, 1H), 8.48 (s, 1H), 8.18-8.17 (d, 2H), 8.02-8.00 (d, 3H), 7.65-7.64 (d, 2H), 7.13-7.11 (d, 2H), 4.08-4.00 (t, 2H), 1.75-1.24 (m, 20H), 0.86-0.83 (t, 3H). Anal. Calcd. for $C_{31}H_{36}N_2O_3$: C, 76.83; H, 7.49; N, 5.78 and found C, 76.02; H, 7.38; N, 5.74. **FT-IR(ATR), υ** cm⁻¹: 2923, 2850 (C-H stretch), 2208 (C≡N stretch), 1664 (C=O stretch), 1599, 1510 (C=C), 1179 (C-N stretch).

Synthesis of (Z)-3-(4-(dodecyloxy)phenyl)-2-(4-((2,4,6-trioxotetrahydropyrimidin-5(2H)-ylidene)methyl)phenyl)acrylonitrile (N₂)

A mixture of intermediate **4** (1 eq) was dissolved in 10-15 mL of absolute methanol and to this mixture 1.2 eq of an active methylene compound like barbituric acid was added under argon atmosphere and heated at 60 ºC with stirring for 10 h. After completion of the reaction, the content was cooled to room temperature and precipitated solid was filtered, washed with cold methanol and collected. It was further recrystallized from CHCl₃-hexane mixture to get a pure product.

Bright red solid, Yield: 74%. Melting point: 342-344ºC. **¹H NMR** (400 MHz, DMSO-d₆, δ ppm): 11.34 (s, 2H), 8.48 (s, 1H), 8.19-8.18 (d, 2H), 8.02-8.00 (d, 3H), 7.65-7.64 (d, 2H), 7.14-7.11 (d, 2H), 4.09-4.02 (t, 2H), 1.76-1.24 (m, 20H), 0.87-0.83 (t, 3H). Anal. Calcd. for $C_{32}H_{37}N_3O_4$: C, 72.84; H, 7.07; N, 7.96; and found C, 72.55; H, 7.63; N, 7.85. **FT-IR(ATR), υ** cm⁻¹: 3203 (N-H stretch), 2944, 2835 (C-H stretch), 2320 (C≡N stretch), 1595, 1522, 1494 (C=C), 1180 (C-N stretch).
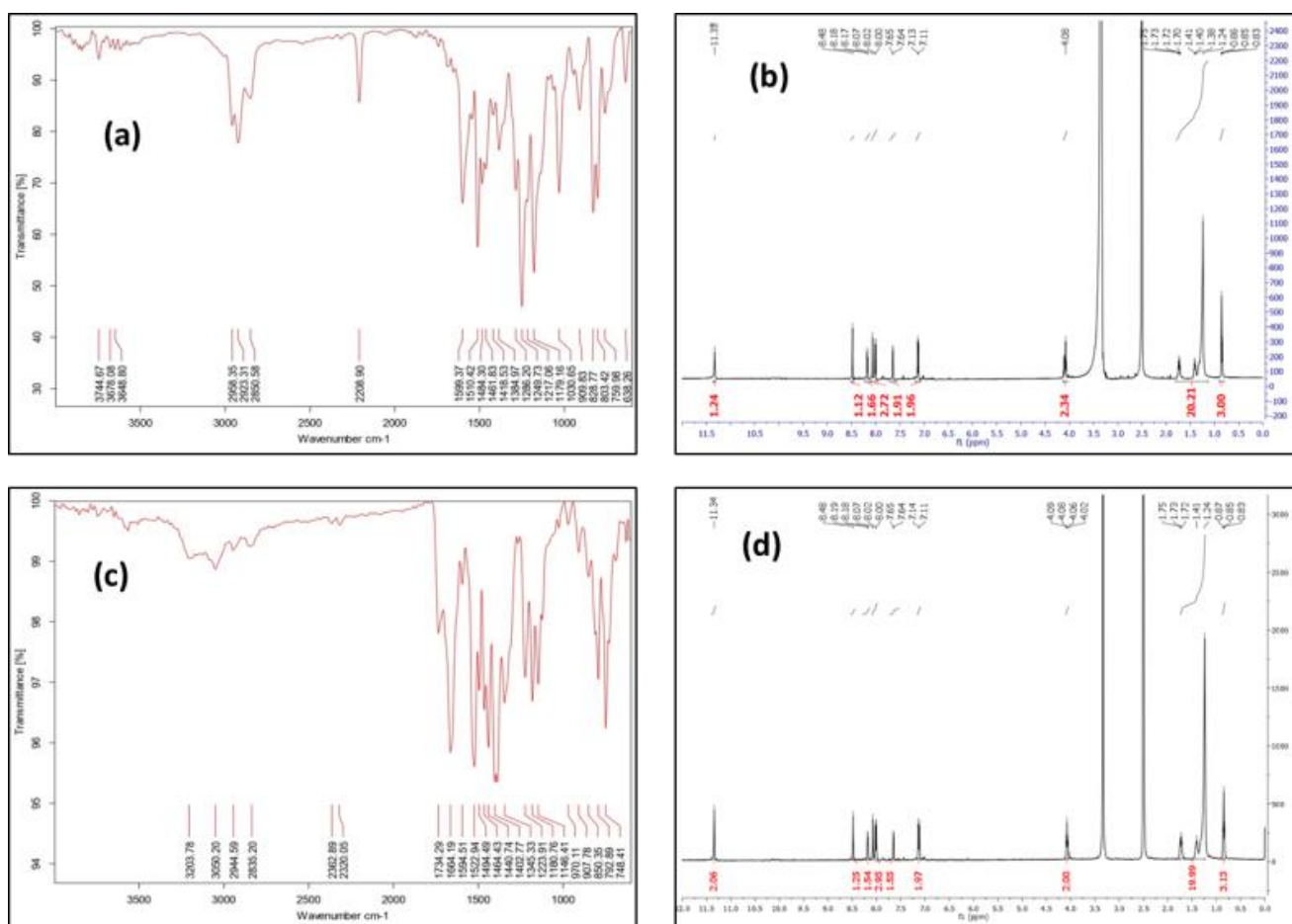
Figure 2. FT-IR spectra of **(a) N₁, (c) N₂** and ¹H-NMR spectra of **(b) N₁, (d) N₂**

4. Results and discussion

4.1 Theoretical studies

To gain a much deeper understanding of the geometrical configurations and frontier molecular orbitals of N_{1-2}, molecular orbital calculations were carried out using the density functional theory (DFT). Turbomole 7.2 software package was used to execute the theoretical calculations. Using a semiempirical AM1 basis with MOPAC in Tmolex, we have optimized the ground state geometries of the dye molecules in a gas phase. Aforesaid geometries were further optimized using C_1 point group symmetry *via* the Becke's three-parameter hybrid functional and Lee-Yang-Parr's gradient-corrected correlation functional (B3LYP) program and basic set def-TZVPP was used for all the calculations.[22,23] The electronic cloud distributions in the FMO levels of dyes N_{1-2} are depicted in **Figures 2** and the corresponding data are summarized in **Table 1**.

As seen from **Figure 2**, in case of HOMO levels, electron densities of N_{1-2} are primarily distributed along with the donor unit, which clearly indicates the electron-donating capacity of dodecyloxyphenyl group along with the phenylene unit. Nevertheless, the electron density distribution in LUMOs is found at the acceptor part, *i.e.* cyanoacetic acid/barbituric acid and π conjugated spacer containing cyanovinylene group. The theoretical HOMO energy levels obtained for dyes N_{1-2} are –6.01 eV (N_1), –6.02 eV (N_2) which are significantly lower than that of the redox potential of I_3^-/I^- electrolyte system (–5.2 eV) confirming the synthesized dyes can undergo a quick ground state regeneration process. The theoretical LUMO energy levels obtained for dyes N_{1-2} are –2.91 eV (N_1), –3.01 eV (N_2) which are significantly higher than the conduction band (CB) of TiO_2 (–4.2 eV) indicating their fast electron injection. The difference in the theoretical bandgap obtained for N_1 and N_2 may be due to the different anchoring abilities of the molecules. Conclusively, the well-overlapped HOMO and LUMO orbitals of the dyes N_{1-2} can guarantee a fast charge transfer between donor and acceptor units and the efficient interfacial injection of electrons from the excited state of the dye molecule into the conduction band of the semiconductor.
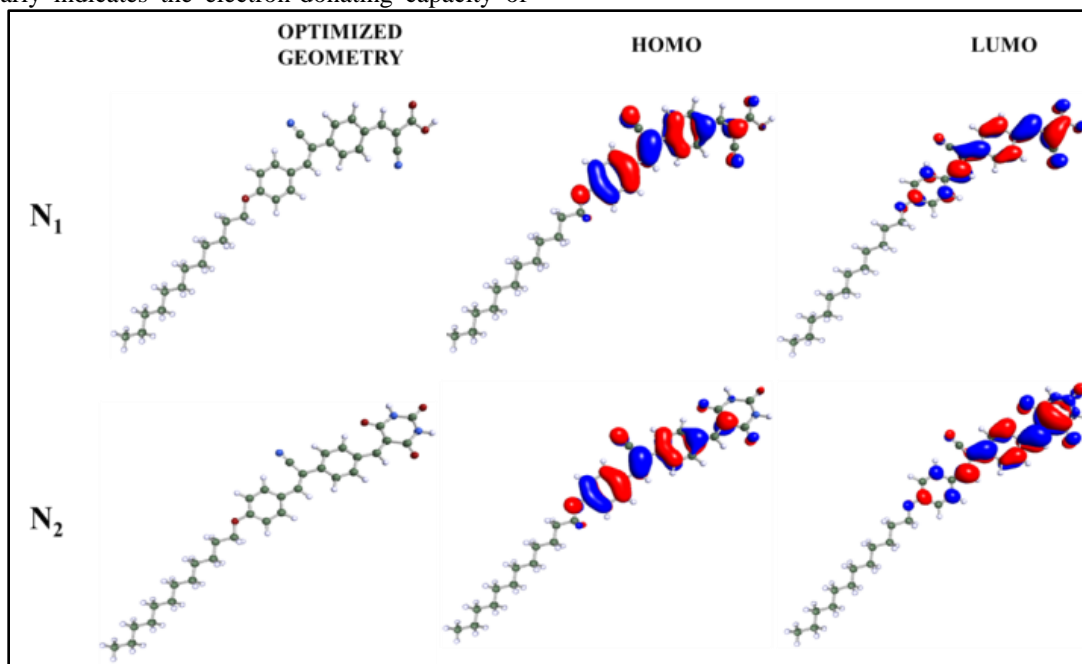
Figure 2. The electronic cloud distributions in the FMO levels of dyes N_{1-2}

Table 1. Theoretical electrochemical data of dyes N_{1-2}

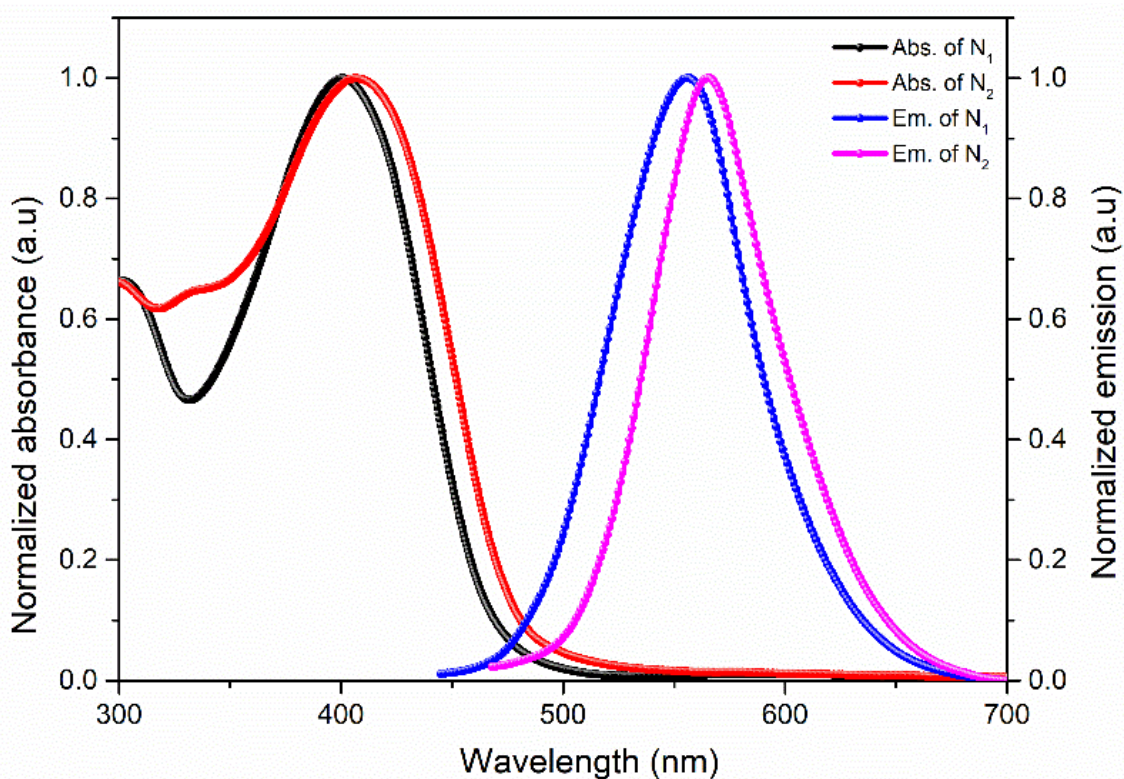| Parameters	N_1	N_2
E_{HOMO} (eV)	–6.01	–6.02
E_{LUMO} (eV)	–2.91	–3.01
[a]E_g (eV)	3.10	3.07

[a]The values obtained in DFT calculations to vacuum

4.2 Photophysical properties

The optical behavior (UV-Visible absorption spectra and fluorescence emission spectra) of the newly synthesized N_{1-2} were recorded in 10^{-5} M DMF solution. Their spectra are displayed in **Figure 3** and their corresponding data are tabulated in **Table 2**. From their spectra, we can conclude that both N_{1-2} exhibit a similar type of absorption profiles and the observed major λ_{max} of N_1 is 401 nm, and that of N_2 is 415 nm, respectively. This is mainly due to the intramolecular charge transfer (ICT) / π-π^* transition of the chromophores between donor and acceptor.[24] From the results, it is clear that the observed bathochromic shift of N_2 when compared to that of N_1 is probably due to the presence of strong electron-withdrawing ability of barbituric acid.

Further, from the PL spectral results, it is clear that both the molecules exhibit solid luminescence maxima in the region of 550-570 nm. The molecule N_1 displays λ_{emi} of 554 nm that is slightly blue-shifted compared to that of N_2 (568 nm). In continuation, the optical bandgap and Stoke shifts were estimated from the intersection between normalized absorption and emission spectra.[25] Also, from the data, Stoke shift values were determined to be in the range of 6490-6887 cm^{-1}. The calculated bandgaps are 2.59 eV (N_1), and 2.51 eV (N_2). Conclusively, N_1 results in a higher Stoke shift value (6887 cm^{-1}) with appropriate bandgap, which ultimately results in superior dye absorption for the molecule, and thus, it is capable of functioning as a better sensitizer.

Figure 3. Intersection of UV-Vis absorption and fluorescence emission spectra of N_{1-2} recorded in 10^{-5} M DMF solution under ambient atmosphere

Table 2. Photophysical characterization data of N_{1-2}

Parameters	N_1	N_2
λ_{abs}[a] (nm)	401	415
λ_{emi}[b] (nm)	554	568
Stokes shift (nm)	6887	6490
E_{0-0}[c], optical (eV)	2.59	2.51

[a] Absorption spectra measured in DMF (at concentration of 10^{-5} M) at room temperature
[b] Emission spectra measured in DMF (at concentration of 10^{-5} M) at room temperature
[c] Optical band gap E_{0-0} is the voltage of intersection point between absorption and emission   spectra

4.3 Electrochemical characterization

The cyclic voltammetry studies (CV measurements) were performed for **N₁₋₂** to elucidate the energy levels of synthesized molecules for a favourable electron-injection process. The conventional three-electrode system was used to measure the CV parameters, in which platinum disc, glassy carbon, and Ag/AgCl acts as passive, working, and reference electrodes, respectively.[26,27] The tetra *n*-butylammoniumhexafluoro phosphate was used as supporting electrolyte and the potentials were measured at a scan rate of 100 mVs⁻¹ in acetonitrile solution at room temperature and the corresponding voltammograms of **N₁₋₂** are shown in **Figure 4a**. Further, the ground state oxidation potentials (GSOP) of the synthesized molecules were calculated from the onset oxidation potential of the oxidation peak and the values obtained for **N₁₋₂** are tabulated in **Table 3**. Accordingly, the GSOP values of both the molecules were found to be –5.43 and –5.44 eV, *respectively* and it is clear the experimental HOMO values were found to be lower than that of the redox potential of the I_3^-/I^- electrolyte system (-5.2 eV),

suggesting that both the dyes can provide a driving force for their quick ground state regeneration.

The dye **N₁** has the highest positive potential among all, which may be due to the presence of a better electron-donating dodecyloxyphenyl group along with a strong cyanoacetic acid as an electron acceptor. Further, the exited state oxidation potential (ESOP) values were calculated from their ground state oxidation potential (GSOP) values and optical band gaps E_{0-0}. **Table 3** depicts the estimated ESOP values of all the dyes and **Figure 4b** shows the pictorial representation of their energy level diagram. As seen from the table, their ESOPs are –2.84 eV (**N₁**), and –2.93 eV (**N₂**) which are greater than the potential of CB of TiO₂ (–4.2 eV) indicating good electron injection from the excited state of the dye molecule to the CB of the TiO₂.[28] Thus, the dye **N₁** satisfies the stringent requirement which is mandatory for the affirmative transition of charges throughout the photo-electronic conversion cycle. From the results, we can confirm that both **N₁₋₂** have the ability to act as potential candidates for sensitizers in dye-sensitized solar cells.
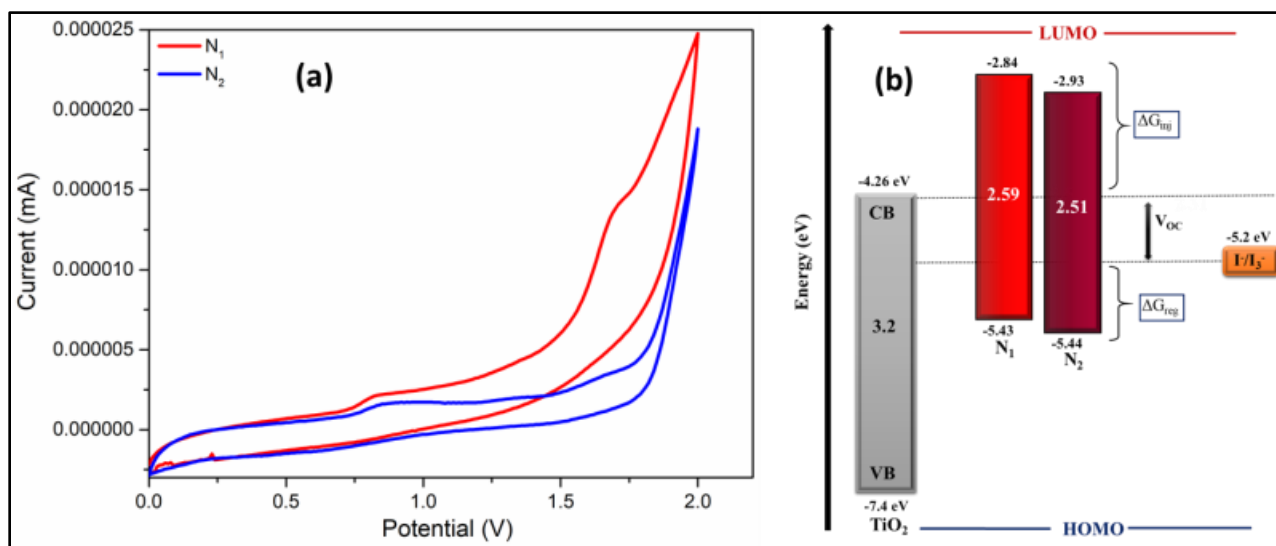
Figure 4. (**a**) Cyclic Voltammograms (CV) of dyes **N₁₋₂**, (**b**) Molecular energy level diagram showing experimental HOMO, LUMO, and bandgap values of **N₁**.

Table 3. Electrochemical characterization data of the dyes **N₁₋₂**

Parameters	N₁	N₂
E_{OX} (V *vs.* NHE)	0.73	0.74
E_{OX}^a (V *vs.* NHE)[#]	–1.86	–1.77
HOMO (eV)[d]	–5.43	–5.44
LUMO (eV)[d]	–2.84	–2.93

7

The E* values were formulated by, $E_{OX}* = E_{OX} - E_{0-0}$. [d] All the potentials were obtained during cyclic voltammetric investigations in 0.1 M Bu_4NPF_6 in DMF, and platinum electrode diameter: 1 mm, sweep rate: 100 mVs^{-1}

5. Conclusion

In summary, we have designed and synthesized two new push-pull type phenylene-based organic chromophores **N$_{1-2}$** carrying dodecyloxyphenyl group as the electron donor, cyanovinylene linked with phenylene system as the π-spacer,

and cyanoacetic acid/barbituric acid as the electron accepto r / anchoring unit. The simplicity of their synthesis from available commercial products and easy purification steps offer a cost-

effective and scalable route. Their photophysical as well as electrochemical properties were probed systematically and the effect of structural modification on their properties has been discussed in-depth. Our results demonstrate that their absorption and emission are in the range of 400-420 nm and 550-570 nm, *respectively* with a bandgap of 2.51-2.59 eV, nearly matching to that of reported sensitizersfor DSSCs. Further, they have been comprehensively evaluated using quantum chemistry simulations on the basis of DFT studies and the results strongly support their high charge transfer efficiency. The results clearly indicate that **N$_{1-2}$** meet the basic prerequisites of an ideal sensitizer, making them highly suitable for DSSC application. Thus, our outcomes provide new design strategies for low-cost and effective photosensitizers, and also offer the guiding principle on the structural design of small organic molecules for sensitization applications.

Declaration of Competing Interest

The authors declare that they have no known competing financial interests or personal relationships that could have appeared to influence the work reported in this paper.

References

1. O'regan, B.; Grätzel, M.A Low-cost, High-Effeciency Solar Cell Based on Dye-Sensitized Colloidal TiO$_2$ Films. Nature. **1991**, 353(6346), 737.

2. Mishra, A.; Fischer, M. K. R.; Bäuerle, P. Metal-Free Organic Dyes for Dye-Sensitized Solar Cells : From Structure : Property Relationships to Design Rules. Angew. Chem . **2009**, 48(14), 2474-2499.

3. Meier, H.; Huang, Z.; Cao, D. New class of Metal-Free Organic Dyes for Efficient dye-sensitized solar cells.J. Mater. Chem. A. **2017**, 5, 9828-9837.

4. Keremane, K. S.; Prathapani, S.; Jia, L.; Bahulayan, D.; Adhikari, A. V.; Priyadarshi, A.; Mhaisalkar, S. G. Solvent Selection for Highly Reproducible Carbon-Based Mixed-Cation Hybrid Lead Halide Perovskite Solar Cells via Adduct Approach. Sol. Energy. **2020**, 199, 761-771.

5. Yang, J.; Ganesan, P.; Teuscher, J.; Moehl, T.; Joo, Y.; Yi, C.; Comte, P.; Pei, K.; Holcombe, T. W.; Mohammad, K.; Hua, J.; Zakeeruddin, S. M.; Tian, H.; Grätzel, M. Influence of the Donor Size in D- # -A Organic Dyes for Dye Sensitized Solar Cells. J. Am. Chem. Soc. **2014,** 136(15), 5722-5730.

6. Warnan, J.; Pellegrin, Y.; Blart, E.; Zhang, L.; Brown, A.; Hammarström, L.; Jacquemin, D.; Odobel, F. Acetylacetone Anchoring Group for NiO-Based Dye-Sensitized Solar Cell. Dyes Pigm. **2014**, 105, 174-179.

7. Das, T. P.; Ilaiyaraja, P.; Sudakar, C. Whispering-Gallery Mode Assisted Enhancement in the Power Conversion Efficiency of DSSC and QDSSC Devices Using TiO Microsphere Photoanodes Whispering-Gallery Mode Assisted Enhancement in the Power Conversion Efficiency of DSSC and QDSSC Devices Using TiO 2 Microsphere Photoanodes. ACS Appl. Energy Mater. **2018**, 1(2), 765-774.

8. Kervella, Y.; Maldivi, P.; Palomares, E.; Demadrille, R. Side Chain Engineering of Organic Sensitizers for Dye-Sensitized Solar Cells : A Strategy to Improve Performances and Stability †. J. Mater. Chem. A **2017**, 5, 6122-6130.

9. Gong, Y.; Cole, J. M.; Ozoe, H.; Kawase, T. Photo-Excited Phenyl Ring Twisting in Quinodimethane Dyes Enhances Photovoltaic Performance in Dye-Sensitized Solar Cells. ACS Appl. Energy Mater. **2018**, 1(3), 1127-1139.

10. Dong, H.; Liang, M.; Xue, S.Twisted Fused-Ring Thiophene Organic Dyes Sensitized Solar Cells. J. Phys. Chem. C. **2016**, 120(40), 22822-22830.

11. Pradhan, A.; Saikiran, M.; Kapil, G.; Hayase, S.; Pandey, S. S. Synthesis and Photophysical Characterization of Unsymmetrical Squaraine Dyes for Dye-Sensitized Solar Cells Utilizing Cobalt Electrolytes. ACS Appl. Energy Mater. **2018**, 1(9), 4545-4553.

12. Warnan, J.; Favereau, L.; Pellegrin, Y.; Blart, E.; Jacquemin, D.; Odobel, F. Compact Diketopyrrolopyrrole Dye as Efficient Sensitizer in Titanium Dioxide Dye-Sensitized Solar Cells. J. Photochem. Photobiol. A **2011**, 226(1), 9–15.

13. Naik, P.; Abdellah, I. M.; Abdel-Shakour, M.; Su, R.; Keremane, K. S.; El-Shafei, A.; VasudevaAdhikari, A. Improvement in Performance of N3 Sensitized DSSCs with

Structurally Simple Aniline Based Organic Co-Sensitizers. Sol. Energy **2018**, 174, 999-1007.

14. Yang, Z.; Liu, C.; Li, K.; Cole, J. M.; Shao, C.; Cao, D. Rational Design of Dithienopicenocarbazole-Based Dyes and a Prediction of Their Energy-Conversion Efficiency Characteristics for Dye-Sensitized Solar Cells. ACS Appl. Energy Mater. **2018**, 1(4), 1435-1444.

15. Mao, L.; Wu, Y.; Jiang, J.; Guo, X.; Heng, P.; Wang, L.; Zhang, J. Rational Design of Phenothiazine-Based Organic Dyes for Dye-Sensitized Solar Cells : The Influence of π-Spacers and Intermolecular Aggregation on Their Photovoltaic Performances. J. Phys. Chem. C. **2020**, 124 (17), 9233-9244.

16. Qian, X.; Shao, L.; Li, H.; Yan, R.; Wang, X.; Hou, L. Dyes for Highly Efficient Dye-Sensitized Solar Cells. J. Power Sources. **2016**, 319, 39-47.

17. Chen, H.; Gong, Y.; Vazquez-mayagoitia, A.; Zhang, J.; Cole, J. M. Dye Aggregation , Photo-Structural Reorganization and Multiple Concurrent Dye \ldots TiO$_2$ Binding Modes in Dye-Sensitized Solar Cell Working Electrodes Containing Benzothiadiazole-Based Dye RK-1. ACS Appl. Energy Mater. **2020**, 3(1), 423-430.

18. Patil, D.; Jadhav, M.; Avhad, K.; Chowdhury, T. H.; Islam, A.; Bedja, I.; Sekar, N. A New Class of Triphenylamine-Based Novel Sensitizers for DSSCs : A Comparative Study of Three Different Anchoring Groups †. New J. Chem. **2018,** 42, 11555–11564.

19. Prakash, G.; Subramanian, K. Interaction of Pyridine p - Bridge-Based Poly(Methacrylate) Dyes for the Fabrication of Dye-Sensitized Solar Cells with the Influence of Different Strength Phenothiazine , Fluorene and Anchoring Mode †. New J. Chem. **2018**, 42, 17939-17949.

20. Naik, P.; Keremane, K. S.; Elmorsy, M. R.; El-shafei, A.; Adhikari, A. V. Carbazole based organic dyes as effective photosensitizers: A comprehensive analysis of their structure-property relationship. Wiley, electrochemical science advances, **2021**, e2100061, DOI: 10.1002/elsa.202100061.

21. Elmorsy, M. R.; Su, R.; Fadda, A. A.; Etman, H. A.; Taw, E. H.; El-shafei, A. Molecular Engineering and Synthesis of Novel Metal-Free Organic Sensitizers with D- π -A- π -A Architecture for DSSC Applications : The effect of the Anchoring Group. Dyes Pigm. **2018**, 158, 121-130.

22. Keremane, K. S.;Rao, R.; and Adhikari, A. V.Simple 3,6-disubstituted carbazoles as potential hole-transport materials: Photophysical, electrochemical and theoretical studies. Photochemistry and Photobiology-Wiley, **2020**, 97, 289-300.

23. Keremane, K. S.; Naik, P.; Adhikari, A. V. Simple Thiophene Based Organic Dyes as Active Photosensitizers for DSSC Application: from Molecular Design to Structure Property Relationship. J. nano electron. phys. 2020, 12, 02039.

24. Keremane, K. S.; Adhikari, A. V. Simple carbazole derivatives with mono/dimethoxyphenyl acetonitrile substituents as hole-transporting materials: Performance studies in hybrid perovskite solar cells. Wiley, electrochemical science advances. **2021**, e2000036. DOI: 10.1002/elsa.202000036.

25. Keremane, K. S.; Abdellah, I. M.; Naik, P.; El-Shafei, A.; Adhikari, A. V. Simple thiophene-bridged D-π-A type chromophores for DSSCs: A comprehensive study on their sensitization and co-sensitization properties. Phys. Chem. Chem. Phys. **2020**, 22, 23169-23184.

26. Naik, P.; Keremane, K. S.; Elmorsy, M. R.; Su, R.; El-shafei, A. Highly efficient Carbazole Based Co-Sensitizers Carrying Electron deficient Barbituric Acid for NCSU-10 Sensitized DSSCs. Sol. Energy. **2018**, 169, 386-391.

27. Mahmood, A.; Hu, J. Y.; Zhou. E. Recent progress of porphyrin-based materials for organic solar cells. J. Mater. Chem. A. **2018**, 6, 16769-16797.

28. Park, J.; Kim, D. W.; Chung, H. Y.; Park, S. Y. conjugated polymer for High-performance organic solar cells with small energy loss and high quantum efficiency. J. Mater. Chem. A. **2017**, 5, 16681-16688.